JOURNAL OF GEOPHYSICAL RESEARCH, VOL. 99, NO. B2, PAGES 2591–2600, FEBRUARY 10, 1994

Theoretical study of nonlinear elastic wave propagation

K. R. McCall
Earth and Environmental Sciences Division, Los Alamos National Laboratory, Los Alamos, New Mexico

Abstract. A theoretical study of the propagation of a plane wave in a material with nonlinear response is presented. We start with the wave equation for an isotropic, homogeneous, elastic solid with cubic anharmonicity in the moduli, accounting for attenuation by introducing complex linear and nonlinear moduli. A heirarchy of equations, ordered in powers of the displacement field, is developed. Using a Green function technique, we solve this set of equations systematically for the displacement field at distance x from the source. We examine the influence of propagation distance, source frequency spectrum, source displacement amplitude, attenuation, and nonlinear coefficient on the spectrum of a propagating wave. The displacement field for various source functions is calculated using parameters typical of rocks.

Introduction

In this paper we consider the nonlinear interaction of frequency components in large-amplitude elastic waves in rocks. Compared to other, more ordered solids, rocks are highly elastically nonlinear. Because of the presence of structural defects such as microcracks and grain boundaries, the effective moduli in rocks change dramatically as a function of stress. The ratio of third-order elastic constants to second-order elastic constants in sandstone is typically orders of magnitude greater than in solids such as iron [*Nazarov et al.*, 1988]. This high degree of nonlinearity means that frequency components mix and energy is transferred from the fundamental frequencies to sum and difference frequencies. We are currently interested in three potential applications of nonlinear effects in rocks. (1) We are interested in modeling of explosion and earthquake sources, where we assume large amounts of energy are transferred from the source frequency spectrum to higher and lower frequencies. The received seismic frequency spectrum may be only distantly related to the original-source frequency spectrum. (2) We are interested in creating a low-frequency seismic source by mixing two high-frequency sources. In general, the lower the frequency desired for a seismic survey, the larger the source must be. (3) We are interested in measuring nonlinear coefficients of highly disordered solids like rocks. Consolidation and saturation conditions cause large deviations in the measured nonlinear coefficients of similar rocks. Therefore accurate measurement of nonlinear terms can be a sensitive measure of consolidation and saturation.

Paper number 93JB02974.
0148-0227/94/93JB-02974$05.00

The purpose of this paper is to develop and illustrate a theoretical framework for investigating these problems that has conceptual clarity and is easy to implement numerically. In the next section we derive the equation of motion for the displacement field from an energy functional that is correct to third order in the strain. We introduce attenuation into the description of the displacement field through a model in which the displacement derivative has instantaneous and retarded (in time) components. This model is discussed in the appendix. The resulting equation of motion for the displacement field lets us classify the forces that drive the displacement field as linear elastic, linear attenuative, nonlinear elastic, or nonlinear attenuative.

We solve the equation of motion for the displacement field by developing the solution in terms of the exact solution of the linear problem. Thus we employ a Green function technique. We illustrate use of this technique in the general solution section, where we work through the case of plane waves propagating with linear elasticity, linear attenuation, nonlinear elasticity (cubic anharmonicity), and nonlinear attenuation. The analytic structure of the equation suggests the following physical description of the phenomena. (1) The system is initially disturbed by an external source, e.g., a transducer at the origin. (2) The Green function describes propagation of the displacement field resulting from this disturbance into the interior of the system. (3) In the interior of the system, the nonlinearity acts on the displacement field to produce an internal source. (4) The Green function works again to carry the displacement consequences of this internal source to the detector.

This physical picture lends itself to generalization. For example, the retarded component of the stress field is quite possibly characterized by a spectrum of relaxation rates [*Day and Minster*, 1984]. The Green function for the corresponding linear problem is relatively complicated. However, there are well-known procedures

for constructing an average Green function that faithfully describes such a circumstance. This Green function can be inserted into the relevant equations in place of the exact Green function with no other changes in the structure of the solution.

The section on specific solution contains a description of a specific Green function for an infinite medium and the resulting displacement components to first order in the nonlinearity. In the section of examples we describe analytical and numerical results for nonlinear wave propagation in two realistic physical situations. In the first example we use a continuous sine wave source to derive an analytic displacement to first order in the nonlinearity. In the limit of low attenuation, these results agree with those of *Polyakova* [1964] and others. In the second example we use a broadband source to study the effect of nonlinear response on seismic propagation. A summary of our conclusions is given in the final section.

Formulation of Problem

The derivation of the equations of motion for a homogeneous solid, including first-order nonlinear elastic terms and linear attenuation, has been described many times. In order to be complete and to fix notation, we sketch a synthesis of the derivations presented by *Landau and Lifshitz* [1959], *Murnaghan* [1951], *Polyakova* [1964], and *Green* [1973].

The equation of motion for elastic wave propagation is

$$\rho\ddot{u}_i = \partial\sigma_{ij}/\partial x_j\,, \tag{1}$$

where ρ is the density of the undeformed solid, u_i is the particle displacement along coordinate i, σ_{ij} is the ij component of the stress tensor, and x_j is the jth coordinate. Conventional summation notation is used. The stress tensor is given by

$$\sigma_{ij} = \frac{\partial\mathcal{E}}{\partial(\partial u_i/\partial x_j)}\,, \tag{2}$$

where $\mathcal{E}$ is the internal energy density of a homogeneous, elastic solid. Including third-order terms in the strain, the internal energy density may be written

$$\mathcal{E} = \frac{\lambda+2\mu}{2}I_1^2 - 2\mu I_2 + \frac{\ell+2m}{3}I_1^3 - 2mI_1I_2 + nI_3\,, \tag{3}$$

where λ and μ are second-order elastic constants (Lamé coefficients); ℓ, m, and n are third-order elastic constants (Murnaghan coefficients); and I_1, I_2, I_3 are the three invariants of the strain tensor:

$$\begin{aligned} I_1 &= \epsilon_{ii}\,,\\ I_2 &= \begin{vmatrix} \epsilon_{22} & \epsilon_{23} \\ \epsilon_{32} & \epsilon_{33} \end{vmatrix} + \begin{vmatrix} \epsilon_{33} & \epsilon_{31} \\ \epsilon_{13} & \epsilon_{11} \end{vmatrix} + \begin{vmatrix} \epsilon_{11} & \epsilon_{12} \\ \epsilon_{21} & \epsilon_{22} \end{vmatrix}\,,\\ I_3 &= \det\epsilon_{ij}\,, \end{aligned} \tag{4}$$

where the components of the strain tensor are given by

$$\epsilon_{ij} = \frac{1}{2}\left(\frac{\partial u_i}{\partial x_j} + \frac{\partial u_j}{\partial x_i} + \frac{\partial u_k}{\partial x_i}\frac{\partial u_k}{\partial u_j}\right). \tag{5}$$

For simplicity, we restrict ourselves to the problem of wave propagation in a single direction, the x direction. Combining (1)–(5) and keeping terms to second order in the displacement field, the equations of motion for the displacement field are [*Gol'dberg*, 1960]:

$$\begin{aligned} \rho\ddot{u}_x &= (\lambda+2\mu)\frac{\partial^2 u_x}{\partial x^2} + S_x' \\ &\quad + \frac{1}{2}[3(\lambda+2\mu)+2(\ell+2m)]\frac{\partial}{\partial x}\left(\frac{\partial u_x}{\partial x}\right)^2 \\ &\quad + \frac{1}{2}(\lambda+2\mu+m)\frac{\partial}{\partial x}\left[\left(\frac{\partial u_y}{\partial x}\right)^2 + \left(\frac{\partial u_z}{\partial x}\right)^2\right], \end{aligned} \tag{6a}$$

$$\begin{aligned} \rho\ddot{u}_y &= \mu\frac{\partial^2 u_y}{\partial x^2} + S_y' \\ &\quad + (\lambda+2\mu+m)\frac{\partial}{\partial x}\left(\frac{\partial u_x}{\partial x}\frac{\partial u_y}{\partial x}\right), \end{aligned} \tag{6b}$$

$$\begin{aligned} \rho\ddot{u}_z &= \mu\frac{\partial^2 u_z}{\partial x^2} + S_z' \\ &\quad + (\lambda+2\mu+m)\frac{\partial}{\partial x}\left(\frac{\partial u_x}{\partial x}\frac{\partial u_z}{\partial x}\right). \end{aligned} \tag{6c}$$

Here $S_i'(x,t)$ is the external source that initiates the response of the system. These equations describe a system having linear and nonlinear elasticity (cubic anharmonicity).

In the frequency domain an explicit Green function can be found for the problem involving linear elasticity and linear attenuation. Therefore define $u_i(x,\omega)$ and $S_i'(x,\omega)$ such that

$$u_i(x,t) = \int_{-\infty}^{\infty}\frac{d\omega}{2\pi}u_i(x,\omega)e^{-i\omega t}\,, \tag{7a}$$

$$S_i'(x,t) = \int_{-\infty}^{\infty}\frac{d\omega}{2\pi}S_i'(x,\omega)e^{-i\omega t}\,. \tag{7b}$$

We introduce attenuation by allowing the spatial derivative of the displacement to have a component that is retarded in time (see the appendix). We let

$$\frac{\partial u_i(x,\omega)}{\partial x} \to \chi(\omega)\frac{\partial u_i(x,\omega)}{\partial x}\,, \tag{8}$$

where

$$\chi(\omega) = 1 - \frac{\Delta}{1-\mathrm{sgn}(\omega)i|\omega\tau|^\nu}\,, \tag{9}$$

Δ can be thought of as the fractional amount of the displacement derivative that is retarded in time ($0 \le \Delta \le 1$), and τ is the characteristic damping time. In the linear case the factor $\chi(\omega)$ is equivalent to the complex factor multiplying real moduli in the standard solid model of a series Voigt unit and spring [*Nowick and Berry*, 1972], that is, $M \to \chi(\omega)M$, where M is a modulus. We have made a generalization of the standard form by adding the power ν.

To be more general, we could allow the complex part of χ to depend on the displacement component. By making the assumption that τ, ν, and Δ are the same for all displacement components, we are making the assumptions that the dimensionless measure of anelasticity Q of the system is the same for both compressional and shear waves and that both types of waves experience the same velocity shift from low to high frequency. Defining $Q^{-1} = -\mathrm{Im}(\chi)/\mathrm{Re}(\chi)$ [*O'Connell and Budiansky*, 1978], we find

$$Q^{-1} = \frac{\mathrm{sgn}(\omega)\Delta|\omega\tau|^{\nu}}{1-\Delta+|\omega\tau|^{2\nu}}. \tag{10}$$

For $\nu = 0$, we find a constant Q result. For $\nu \neq 0$, the linear moduli and Q have low- and high-frequency limits. For low frequencies, $|\omega\tau| \ll 1$,

$$\chi(\omega) \rightarrow (1-\Delta) - \mathrm{sgn}(\omega) i|\omega\tau|^{\nu}\Delta \tag{11a}$$

and $Q^{-1} \rightarrow \mathrm{sgn}(\omega)|\omega\tau|^{\nu}\Delta/(1-\Delta)$. For high frequencies, $|\omega\tau| \gg 1$,

$$\chi(\omega) \rightarrow 1 - \mathrm{sgn}(\omega) i|\omega\tau|^{-\nu}\Delta \tag{11b}$$

and $Q^{-1} \rightarrow \mathrm{sgn}(\omega)|\omega\tau|^{-\nu}\Delta$. In both limits the linear moduli have a small residual complex component. At low frequency the real linear moduli are a factor of $1-\Delta$ smaller than at high frequency. The parameters Δ, τ, and ν may be derived from measurements of Q^{-1} as a function of frequency.

General Solution Using Green Function

We write the equations of longitudinal (L) and transverse (T) motion, (6a)–(6c), in the frequency domain by using the relation for attenuation in (8), the Fourier transforms of (7a) and (7b), and the convolution theorem for Fourier transforms. The equations of motion are

$$\begin{aligned} g_L^{-1}(x,\omega)u_x(x,\omega) &= -S_x(x,\omega) \\ &-\beta\frac{\partial}{\partial x}\int\frac{d\omega'}{2\pi}\chi(\omega')\chi(\phi)\frac{\partial u_x(x,\omega')}{\partial x}\frac{\partial u_x(x,\phi)}{\partial x} \\ &-\gamma\frac{\partial}{\partial x}\int\frac{d\omega'}{2\pi}\chi(\omega')\chi(\phi)\left[\frac{\partial u_y(x,\omega')}{\partial x}\frac{\partial u_y(x,\phi)}{\partial x}\right. \\ &\left.+\frac{\partial u_z(x,\omega')}{\partial x}\frac{\partial u_z(x,\phi)}{\partial x}\right], \end{aligned} \tag{12a}$$

$$\begin{aligned} g_T^{-1}(x,\omega)u_y(x,\omega) &= -S_y(x,\omega) \\ &-2\gamma\frac{c_L^2}{c_T^2}\frac{\partial}{\partial x}\int\frac{d\omega'}{2\pi}\chi(\omega')\chi(\phi)\frac{\partial u_x(x,\omega')}{\partial x}\frac{\partial u_y(x,\phi)}{\partial x}, \end{aligned} \tag{12b}$$

$$\begin{aligned} g_T^{-1}(x,\omega)u_z(x,\omega) &= -S_z(x,\omega) \\ &-2\gamma\frac{c_L^2}{c_T^2}\frac{\partial}{\partial x}\int\frac{d\omega'}{2\pi}\chi(\omega')\chi(\phi)\frac{\partial u_x(x,\omega')}{\partial x}\frac{\partial u_z(x,\phi)}{\partial x}, \end{aligned} \tag{12c}$$

where

$$g_L^{-1}(x,\omega) = \chi(\omega)\frac{\partial^2}{\partial x^2} + k_L^2, \tag{13a}$$

$$g_T^{-1}(x,\omega) = \chi(\omega)\frac{\partial^2}{\partial x^2} + k_T^2, \tag{13b}$$

$$\beta = \frac{3(\lambda+2\mu)+2(\ell+2m)}{2(\lambda+2\mu)}, \tag{14a}$$

$$\gamma = \frac{\lambda+2\mu+m}{2(\lambda+2\mu)}, \tag{14b}$$

$k_L^2 = \omega^2/c_L^2$, $k_T^2 = \omega^2/c_T^2$, $c_L^2 = (\lambda+2\mu)/\rho$, $c_T^2 = \mu/\rho$, $S_i = S_i'/(\lambda+2\mu)$, and $\phi = \omega - \omega'$. The linear terms in the equations of motion, (12a)–(12c), are on the left-hand side in the operators g_L^{-1} and g_T^{-1}. The right-hand sides of (12a)–(12c) have two kinds of sources, the external sources $S_i(x,\omega)$ and the internal sources due to the nonlinearity.

To obtain a systematic Green function solution to (12a)–(12c), we use a parameter η ($0 < \eta \leq 1$) to keep track of powers of the internal source. We expand the displacement and source functions in powers of η;

$$u_i(x,\omega) = u_i^{(0)}(x,\omega) + \eta u_i^{(1)}(x,\omega) + \eta^2 u_i^{(2)}(x,\omega) + \ldots, \tag{15a}$$

$$f_i(x,\omega) = f_i^{(0)}(x,\omega) + \eta f_i^{(1)}(x,\omega) + \eta^2 f_i^{(2)}(x,\omega) + \ldots, \tag{15b}$$

where $f_i^{(0)}(x,\omega)$ is the external source function $S_i(x,\omega)$. In the examples we set $\eta \equiv 1$ and consider only cases where $|u_i^{(n+1)}|/|u_i^{(n)}| < 1$ and the expansion for u_i is convergent. The first few terms in the expansion of the source function are given by

$$f_x^{(0)}(x,\omega) = S_x(x,\omega), \tag{16a}$$

$$\begin{aligned} f_x^{(1)}(x,\omega) &= \frac{\partial}{\partial x}\int\frac{d\omega'}{2\pi}\chi(\omega')\chi(\phi)\left\{\gamma\left[\frac{\partial u_y^{(0)}(x,\omega')}{\partial x}\right.\right. \\ &\left.\cdot\frac{\partial u_y^{(0)}(x,\phi)}{\partial x} + \frac{\partial u_z^{(0)}(x,\omega')}{\partial x}\frac{\partial u_z^{(0)}(x,\phi)}{\partial x}\right] \\ &\left.+\beta\frac{\partial u_x^{(0)}(x,\omega')}{\partial x}\frac{\partial u_x^{(0)}(x,\phi)}{\partial x}\right\}, \end{aligned} \tag{16b}$$

$$\begin{aligned} f_x^{(2)}(x,\omega) &= \frac{\partial}{\partial x}\int\frac{d\omega'}{2\pi}\chi(\omega')\chi(\phi)\left\{2\gamma\left[\frac{\partial u_y^{(0)}(x,\omega')}{\partial x}\right.\right. \\ &\left.\cdot\frac{\partial u_y^{(1)}(x,\phi)}{\partial x} + \frac{\partial u_z^{(0)}(x,\omega')}{\partial x}\frac{\partial u_z^{(1)}(x,\phi)}{\partial x}\right] \\ &\left.+2\beta\frac{\partial u_x^{(0)}(x,\omega')}{\partial x}\frac{\partial u_x^{(1)}(x,\phi)}{\partial x}\right\}, \end{aligned} \tag{16c}$$

$$f_y^{(0)}(x,\omega) = S_y(x,\omega), \tag{16d}$$

$$\begin{aligned} f_y^{(1)}(x,\omega) &= \frac{\partial}{\partial x}\int\frac{d\omega'}{2\pi}\chi(\omega')\chi(\phi) \\ &\cdot 2\gamma\frac{c_L^2}{c_T^2}\frac{\partial u_x^{(0)}(x,\omega')}{\partial x}\frac{\partial u_y^{(0)}(x,\phi)}{\partial x}, \end{aligned} \tag{16e}$$

$$f_y^{(2)}(x,\omega) = \frac{\partial}{\partial x}\int \frac{d\omega'}{2\pi}\chi(\omega')\chi(\phi)2\gamma\frac{c_L^2}{c_T^2}\left[\frac{\partial u_x^{(0)}(x,\omega')}{\partial x}\cdot\frac{\partial u_y^{(1)}(x,\phi)}{\partial x} + \frac{\partial u_x^{(1)}(x,\omega')}{\partial x}\frac{\partial u_y^{(0)}(x,\phi)}{\partial x}\right], \tag{16f}$$

etc. Equating like powers of η, we obtain a hierarchy of equations that allows us to solve for the displacement field to any desired order:

$$g_L^{-1}(x,\omega)u_x^{(n)}(x,\omega) = -f_x^{(n)}(x,\omega), \tag{17a}$$

$$g_T^{-1}(x,\omega)u_j^{(n)}(x,\omega) = -f_j^{(n)}(x,\omega), \quad j = y,z. \tag{17b}$$

Note that to solve for each successive order in the displacement, we require knowledge of all preceding solutions. For example, the source function for $u_x^{(2)}$ is determined by $u_x^{(0)}$, $u_x^{(1)}$, $u_y^{(0)}$, $u_y^{(1)}$, $u_z^{(0)}$, and $u_z^{(1)}$.

Equations (17a) and (17b) can be solved analytically using the Green function that satisfies

$$g_\iota^{-1}(x,\omega)g_\iota(x,x',\omega) = -\delta(x-x'), \quad \iota = L,T, \tag{18}$$

and the appropriate value of k ($k_L = \omega/c_L$ for u_x and $k_T = \omega/c_T$ for u_y and u_z). These Green functions are used to solve (17a) and (17b) for the displacement fields in the form of an integral over a product of a Green function and a source function:

$$u_i^{(n)}(x,\omega) = \int dx' g_\iota(x,x',\omega)f_i^{(n)}(x',\omega), \quad \iota = L,T. \tag{19}$$

The total displacement to order n in frequency space is the sum of n terms $u_i(x,\omega) = u_i^{(0)}(x,\omega) + u_i^{(1)}(x,\omega) + \ldots + u_i^{(n)}(x,\omega)$, where $\eta \to 1$ in (15a). For example, if $S_y = S_z = 0$ and $S_x = S(x',\omega)$, then the first two terms in $u_x(x,\omega)$ are

$$u_x^{(0)}(x,\omega) = \int dx' g_L(x,x',\omega)S(x',\omega), \tag{20a}$$

$$u_x^{(1)}(x,\omega) = \beta\int dx' g_L(x,x',\omega)\int \frac{d\omega'}{2\pi}\chi(\omega')\chi(\phi)\cdot\frac{\partial}{\partial x'}\left[\int dx''\frac{\partial g_L(x',x'',\omega')}{\partial x'}S(x'',\omega')\cdot\int dx'''\frac{\partial g_L(x',x''',\phi)}{\partial x'}S(x''',\phi)\right]. \tag{20b}$$

The Green function method of solution has conceptual clarity and flexibility. Pictorially, (20a), (20b), and the analog for $u_x^{(2)}$ for a purely compressional source are illustrated in Figure 1. We read (20b) from right to left and relate the equation to u_1 in Figure 1. We see that the linear Green function acts on the source to propagate two separate waves from the source location to point x', the integral on ω' causes the frequency spectra of the two waves to interact with strength β, the Green function propagates the resulting source from x' to x (the point of observation), and the integral on x' sums the results for interactions occurring all along the wave propagation path. The solution has flexibility in that it works for an arbitrary source, allowing one to choose an explicit Green function for a specific geometry or an empirical Green function derived from experiment.

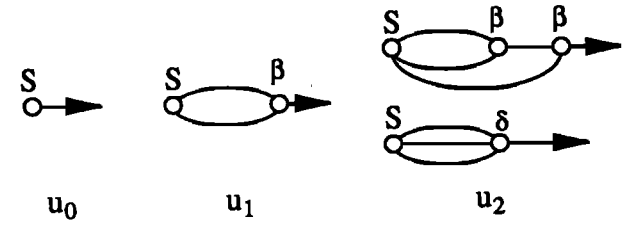

Figure 1. Pictorial description of Green function method. The displacement is the sum of terms $u = u_0+u_1+u_2+\ldots$, where u_0 is the linear component of the displacement given by a Green function propagating a source. The first-order nonlinear term u_1 is given by the Green function propagating two waves from the source that interact with strength β. The Green function then propagates the result of the interaction. The second-order nonlinear term u_2 (for a compressional source) has two terms resulting from the Green function propagating three waves: (1) all three interact with strength δ; or (2) two interact with strength β, propagate, and interact with the third with strength β. In both cases the Green function propagates the result of the interaction to the point of observation x.

Specific Solution

Specific solutions to (19) depend on our choices of Green function and external source. We have chosen to study the same geometry (an infinite solid) and therefore to use the same Green function for all of the examples described in the next section. Nevertheless, the examples apply to a broad range of problems depending on the external source and the physical characteristics to be studied.

The solution to (18) for the Green function of an infinite medium is

$$g_\iota(x,x',\omega) = \frac{i}{2A_\iota(\omega)\chi(\omega)}e^{iA_\iota(\omega)|x-x'|}, \quad \iota = L,T, \tag{21}$$

where

$$A_\iota(\omega) = \kappa_\iota(\omega) + i\alpha_\iota(\omega), \tag{22a}$$

$$\kappa_\iota(\omega) = k_\iota\sqrt{\frac{r+s}{2\left[(1-\Delta)^2+|\omega\tau|^{2\nu}\right]}}, \tag{22b}$$

$$\alpha_\iota(\omega) = |k_\iota|\sqrt{\frac{r-s}{2\left[(1-\Delta)^2+|\omega\tau|^{2\nu}\right]}}, \tag{22c}$$

$$r = \sqrt{s^2+|\omega\tau|^{2\nu}\Delta^2}, \tag{22d}$$

$$s = (1-\Delta)+|\omega\tau|^{2\nu}. \tag{22e}$$

The functions $\kappa_\iota(\omega)$ and $\alpha_\iota(\omega)$, (22b) and (22c), define the dispersion relation and the attenuation in the system. If $\Delta = 0$, then $\kappa_\iota = k_\iota$, $\alpha_\iota = 0$ and we recover the Green function for propagation in an infinite medium in the absence of attenuation. The following asymptotic expressions for $\kappa_\iota(\omega)$ and $\alpha_\iota(\omega)$ can be derived:

$$\begin{array}{ll} \kappa_\iota/k_\iota \to 1/\sqrt{1-\Delta}, & |\omega\tau| \ll 1, \\ \kappa_\iota/k_\iota \to 1, & |\omega\tau| \gg 1, \\ \alpha_\iota/|k_\iota| \to |\omega\tau|^\nu \Delta/2(1-\Delta)^{3/2}, & |\omega\tau| \ll 1, \\ \alpha_\iota/|k_\iota| \to |\omega\tau|^{-\nu}\Delta/2, & |\omega\tau| \gg 1. \end{array} \tag{23}$$

As we pass from $|\omega\tau| \ll 1$ through $|\omega\tau| = 1$ to $|\omega\tau| \gg 1$, the normalized wave vector changes from one constant value to a lower constant value, while the normalized attenuation changes from an $|\omega|^\nu$ dependence to an $|\omega|^{-\nu}$ dependence.

Given the Green function in (21) and the source functions in (16a)–(16f), the solution for the displacement field begins with the terms involving the external sources $f_i^{(0)}(x,\omega)$. Since the y and z directions are identical by symmetry, we choose $f_z^{(0)}(x,\omega) = 0$ and write $f_x^{(0)}(x,\omega)$ and $f_y^{(0)}(x,\omega)$ as sources at the origin of the form

$$f_x^{(0)}(x,\omega) = -2i\chi(\omega)A_L(\omega)U_L\delta(x)F(\omega), \tag{24a}$$

$$f_y^{(0)}(x,\omega) = -2i\chi(\omega)A_T(\omega)U_T\delta(x)F(\omega), \tag{24b}$$

where U_L and U_T are the longitudinal and transverse displacement fields produced at the origin by the source, and $F(\omega)$ is the frequency spectrum of the source with units of time. Substituting $f_i^{(0)}(x,\omega)$ into (19), we find that the linear components of the displacement are

$$u_x^{(0)}(x,\omega) = U_L\, e^{iA_L(\omega)|x|}F(\omega), \tag{25a}$$

$$u_y^{(0)}(x,\omega) = U_T\, e^{iA_T(\omega)|x|}F(\omega), \tag{25b}$$

$$u_z^{(0)}(x,\omega) = 0. \tag{25c}$$

The source functions $f_i^{(1)}$, (16b) and (16e), for the first-order nonlinear displacement terms are determined by the linear displacement terms in (25a)–(25c). These first-order source functions yield first-order nonlinear displacements of the form

$$u_x^{(1)}(x,\omega) = \beta U_L^2 x\, E_{LL}(x,\omega) + \gamma U_T^2 x\, E_{TT}(x,\omega), \tag{26a}$$

$$u_y^{(1)}(x,\omega) = \gamma U_L U_T x \frac{2c_L^2}{c_T^2} E_{LT}(x,\omega), \tag{26b}$$

$$u_z^{(1)}(x,\omega) = 0, \tag{26c}$$

where

$$E_{LL}(x,\omega) = \int \frac{d\omega'}{2\pi} \frac{e^{i[A_L(\omega')+A_L(\phi)]|x|} - e^{iA_L(\omega)|x|}}{i[A_L(\omega')+A_L(\phi)-A_L(\omega)]|x|} \cdot C_{LL}(\omega,\omega')F(\omega')F(\phi), \tag{27a}$$

$$E_{TT}(x,\omega) = \int \frac{d\omega'}{2\pi} \frac{e^{i[A_T(\omega')+A_T(\phi)]|x|} - e^{iA_L(\omega)|x|}}{i[A_T(\omega')+A_T(\phi)-A_L(\omega)]|x|} \cdot C_{TT}(\omega,\omega')F(\omega')F(\phi), \tag{27b}$$

$$E_{LT}(x,\omega) = \int \frac{d\omega'}{2\pi} \frac{e^{i[A_L(\omega')+A_T(\phi)]|x|} - e^{iA_T(\omega)|x|}}{i[A_L(\omega')+A_T(\phi)-A_T(\omega)]|x|} \cdot C_{LT}(\omega,\omega')F(\omega')F(\phi), \tag{27c}$$

and

$$C_{LL}(\omega,\omega') = \frac{A_L(\omega')A_L(\phi)[A_L(\omega')+A_L(\phi)]}{A_L(\omega')+A_L(\phi)+A_L(\omega)} \cdot \frac{\chi(\omega')\chi(\phi)}{\chi(\omega)}, \tag{28a}$$

$$C_{TT}(\omega,\omega') = \frac{A_T(\omega')A_T(\phi)[A_T(\omega')+A_T(\phi)]}{A_T(\omega')+A_T(\phi)+A_L(\omega)} \cdot \frac{\chi(\omega')\chi(\phi)}{\chi(\omega)}, \tag{28b}$$

$$C_{LT}(\omega,\omega') = \frac{A_L(\omega')A_T(\phi)[A_L(\omega')+A_T(\phi)]}{A_L(\omega')+A_T(\phi)+A_T(\omega)} \cdot \frac{\chi(\omega')\chi(\phi)}{\chi(\omega)}. \tag{28c}$$

The results in (26a) and (26b) are arranged in the form of the product of an amplitude with a frequency-dependent envelope function. For example, the amplitude proportional to γ in (26a) is proportional to U_T^2, as it is due to two transverse waves launched by the transverse source, and proportional to x, as the internal source works at all points between the point of observation and the external source point $x = 0$. The other amplitude factors can be understood in the same way. The envelope functions $E(x,\omega)$ describe the decay of the amplitude due to attenuation. For example, $E_{TT}(x,\omega)$ in (26a) contains the degradation of the strength of the internal source due to attenuation of the transverse displacement fields causing the source (the factor $\exp\{-[\alpha_T(\omega') + \alpha_T(\phi)]|x|\}$) and attenuation of the displacement field between the internal source point and the point of detection (the factor $\exp -\alpha_L(\omega)|x|$).

In the limit of no attenuation, that is, $\chi(\omega) \equiv 1$, the envelope functions become

$$E_{LL}(x,\omega) = \int \frac{d\omega'}{2\pi} \frac{k_L'(k_L - k_L')}{2} F(\omega')F(\phi)e^{ik_L|x|}, \tag{29a}$$

$$E_{TT}(x,\omega) = \int \frac{d\omega'}{2\pi} \frac{k_T'k_T(k_T - k_T')}{i(k_T^2 - k_L^2)|x|} F(\omega')F(\phi) \cdot \left(e^{ik_T|x|} - e^{ik_L|x|}\right), \tag{29b}$$

$$E_{LT}(x,\omega) = \int \frac{d\omega'}{2\pi} \frac{k_L'(k_T - k_T')(k_L' + k_T - k_T')}{i(k_L' - k_T' + 2k_T)(k_L' - k_T')|x|} \cdot F(\omega')F(\phi)\left(e^{i(k_L'+k_T-k_T')|x|} - e^{ik_T|x|}\right), \tag{29c}$$

where $k' = \omega'/c$. Note that the linear x dependence of the amplitudes in (26a) and (26b) will cancel with the

x dependence of the envelope functions in all but the longitudinal-longitudinal wave interaction (E_{LL}).

Examples

Continuous Single-Frequency Sine Wave

As the first example we choose the external driving force to be a continuous single-frequency compressional sine wave at the origin with displacement amplitude U. That is, in (24a) and (24b), let $U_L = U$, $U_T = 0$, and

$$F(\omega) = 2\pi \frac{1}{2i}[\delta(\omega - \omega_0) - \delta(\omega + \omega_0)]. \quad (30)$$

Displacement occurs only in the x direction.

From (25a) and (7a), the linear displacement is

$$u_x^{(0)}(x,t) = \frac{U}{2i}\left[e^{i[A_L(\omega_0)|x| - \omega_0 t]} - e^{i[A_L(-\omega_0)|x| + \omega_0 t]}\right]. \quad (31a)$$

Equation (31a) reduces to a sine wave modified by an exponentially decaying envelope in both the high- and low-frequency limits:

$$u_x^{(0)}(x,t) \to U e^{-\alpha_m|x|}\sin(k_m|x| - \omega_0 t), \quad (31b)$$

where

$$\begin{array}{ll} k_m = k_P = \omega_0/c_L\sqrt{1-\Delta}, & |\omega\tau| \ll 1, \\ k_m = k_0 = \omega_0/c_L, & |\omega\tau| \gg 1, \\ \alpha_m = \alpha_P = k_P(\omega_0\tau)^\nu \Delta/2(1-\Delta), & |\omega\tau| \ll 1, \\ \alpha_m = \alpha_H = k_0(\omega_0\tau)^{-\nu}\Delta/2, & |\omega\tau| \gg 1. \end{array} \quad (32)$$

From (26a) and (7a), the first-order nonlinear displacement is

$$u_x^{(1)}(x,t) = -\frac{\beta U^2 x}{4}\left[\frac{|\chi(\omega_0)A_L(\omega_0)|^2}{\chi(0)}\frac{1 - e^{-2\alpha_L(\omega_0)|x|}}{2\alpha_L(\omega_0)|x|} + \frac{4}{|x|}Im\left\{\frac{\chi^2(\omega_0)A_L^3(\omega_0)}{\chi(2\omega_0)}\frac{e^{i2A_L(\omega_0)|x|} - e^{iA_L(2\omega_0)|x|}}{4A_L^2(\omega_0) - A_L^2(2\omega_0)}\right\}\right]. \quad (33a)$$

At low and high frequencies, (33a) reduces to the sum of a cosine at $2\omega_0$ and a zero frequency term. Both terms are modified by attenuative exponentials. In the limit $\omega_0\tau \ll 1$,

$$u_x^{(1)}(x,t) \to -\frac{\beta U^2 k_0^2 x}{4}\left[\frac{1 - e^{-2\alpha_P|x|}}{2\alpha_P|x|} + \frac{e^{-2\alpha_P|x|} - e^{-2^{1+\nu}\alpha_P|x|}}{2(2^\nu - 1)\alpha_P|x|}\cos(2k_P|x| - 2\omega_0 t)\right], \quad (33b)$$

in agreement with the results of *Polyakova* [1964]. In the limit $\omega_0\tau \gg 1$,

$$u_x^{(1)}(x,t) \to -\frac{\beta U^2 k_0^2 x}{4}\left[\frac{1 - e^{-2\alpha_H|x|}}{2(1-\Delta)\alpha_H|x|} + \frac{e^{-2^{1-\nu}\alpha_H|x|} - e^{-2\alpha_H|x|}}{2(1-2^{-\nu})\alpha_H|x|}\cos(2k_0|x| - 2\omega_0 t)\right]. \quad (33c)$$

In Figure 2, we show the transition of the first-order nonlinear term from $\omega_0\tau \ll 1$ to $\omega_0\tau \gg 1$ at three distances from the source. The normalized $u_x^{(1)}(x,t)$ values from (33a), (33b), and (33c) are shown as a function of $\omega_0\tau$ for a source frequency of 10 Hz. The parameter values are $c = 6000$ m/s; $\Delta = 0.2$; $\nu = 1$; and $x = 0.6$, 6, and 60 km. Since the source is continuous, we chose $t = 0$. The dashed curves in Figure 2 are the $\omega_0\tau \ll 1$ results; the dotted curves are the $\omega_0\tau \gg 1$ results.

In the absence of attenuation ($\alpha x \ll 1$) we have the familiar result

$$u_x(x,t) = u_x^{(0)} + u_x^{(1)} = U\sin(k_0|x| - \omega_0 t) - \frac{\beta U^2 k_0^2 x}{4}[1 + \cos(2k_0|x| - 2\omega_0 t)], \quad (34)$$

to first order in the nonlinearity. Thus the displacement amplitude of the $2\omega_0$ harmonic grows as the square of the amplitude of the fundamental, the square of the frequency, linearly with distance, and linearly with the material parameter β.

For the case discussed here of displacement due to a compressional source in the x direction, the equation of

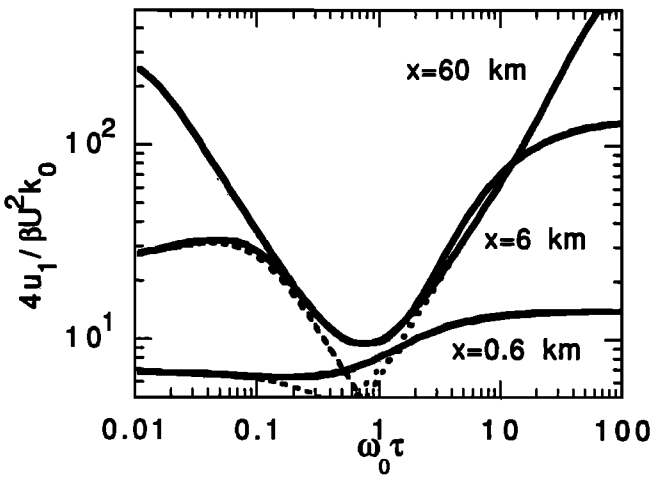

Figure 2. Attenuation dependence of the first-order nonlinear displacement. The normalized first-order nonlinear displacement is shown as a function of $\omega_0\tau$. The solid curves are calculated from (33a) at distances $x = 0.6$, 6, and 60 km. The source frequency is 10 Hz, $\Delta = 0.2$, and $\nu = 1$. The value of τ is varied. The dashed curves are the low $\omega_0\tau$ limit, (33b); the dotted curves are the high $\omega_0\tau$ limit, (33c). The crossover from low to high $\omega_0\tau$ and the point of maximum attenuation are at $\omega_0\tau \approx 1$.

motion (6a) may be easily expanded to include quartic anharmonicity as well as cubic anharmonicity:

$$\frac{1}{c_L^2}\ddot{u}_x = \frac{\partial}{\partial x}\left[\frac{\partial u_x}{\partial x} + \beta\left(\frac{\partial u_x}{\partial x}\right)^2 + \delta\left(\frac{\partial u_x}{\partial x}\right)^3\right] + S_x\,, \tag{35}$$

where β and δ are measures of the strength of the cubic and quartic anharmonicity, respectively. Given the equation of motion in (35), the second-order source function $f_x^{(2)}$ becomes

$$f_x^{(2)}(x,\omega) = \frac{\partial}{\partial x}\int \frac{d\omega'}{2\pi}\chi(\omega')\left[\delta\frac{\partial u_x^{(0)}(x,\omega')}{\partial x}\right.$$
$$\cdot\int \frac{d\omega''}{2\pi}\chi(\omega'')\chi(\psi)\frac{\partial u_x^{(0)}(x,\omega'')}{\partial x}\frac{\partial u_x^{(0)}(x,\psi)}{\partial x}$$
$$\left.+2\beta\chi(\phi)\frac{\partial u_x^{(0)}(x,\omega')}{\partial x}\frac{\partial u_x^{(1)}(x,\phi)}{\partial x}\right], \tag{36}$$

where $\psi = \omega - \omega' - \omega''$. In the absence of attenuation, the source function (36) leads to a second-order nonlinear displacement:

$$u_x^{(2)}(x,t) = \frac{U^3k_0^3}{8}\left[(4\beta^2 - 3\delta)\,|x|\cos(k_0|x| - \omega_0 t)\right.$$
$$+\left(\frac{3\delta}{k_0} - \frac{4\beta^2}{k_0} - \beta^2k_0x^2\right)\sin(k_0|x| - \omega_0 t)$$
$$+\left(\frac{\delta}{3k_0} - \frac{4\beta^2}{9k_0} - \beta^2k_0x^2\right)\sin(3k_0|x| - 3\omega_0 t)$$
$$\left.+\left(\frac{4\beta^2}{3} - \delta\right)|x|\cos(3k_0|x| - 3\omega_0 t)\right]. \tag{37}$$

The interactions producing the displacement of (37) are illustrated in Figure 1. The second-order nonlinear displacement has components at ω_0 and $3\omega_0$. The displacement amplitude grows as the cube of the amplitude of the fundamental and the cube of the frequency. At a large propagation distance, the displacement amplitude depends on the square of β and the square of the propagation distance. Note that the quartic anharmonic coefficient δ must be of the order β^2 in order to make a significant contribution to the second order nonlinear displacement. From a literature study of velocity versus pressure data on a variety of rock types, this seems to be the case ($\delta \approx \beta^2$) (G. D. Meegan, Jr., unpublished data, 1993).

In Figure 3 we show the displacement amplitudes of each frequency component in (34) and (37). Figure 3*a* is a plot of the amplitude at the source frequency and the first two harmonics as a function of propagation distance. Figure 3*b* is a plot of the amplitude as a function of the source frequency. The first harmonic ($2f$) grows linearly with propagation distance and as the square of the source frequency; the second harmonic ($3f$) grows as the square of the propagation distance and as the fourth power of the source frequency. The parameters used in the calculation are $U = 5\times10^{-4}$ m (corresponding to strains of order 10^{-6}), $c_L = 6000$ m/s, $\beta = -10^3$ [*Meegan et al.*, 1993], and $\delta = -10^6$. In Figure 3*a* the frequency f is 3 Hz, and in Figure 3*b* the propagation distance x is 10 km. Attenuation is not included.

Broadband Source

A seismic source produces a broadband frequency spectrum. In order to explore whether nonlinear effects modify seismic spectra significantly, we chose $U_L = U$ and $U_T = 0$ in (24a) and (24b) and use

$$F(\omega) = \frac{\Omega}{(i\omega - \Omega)^2}\,, \tag{38a}$$

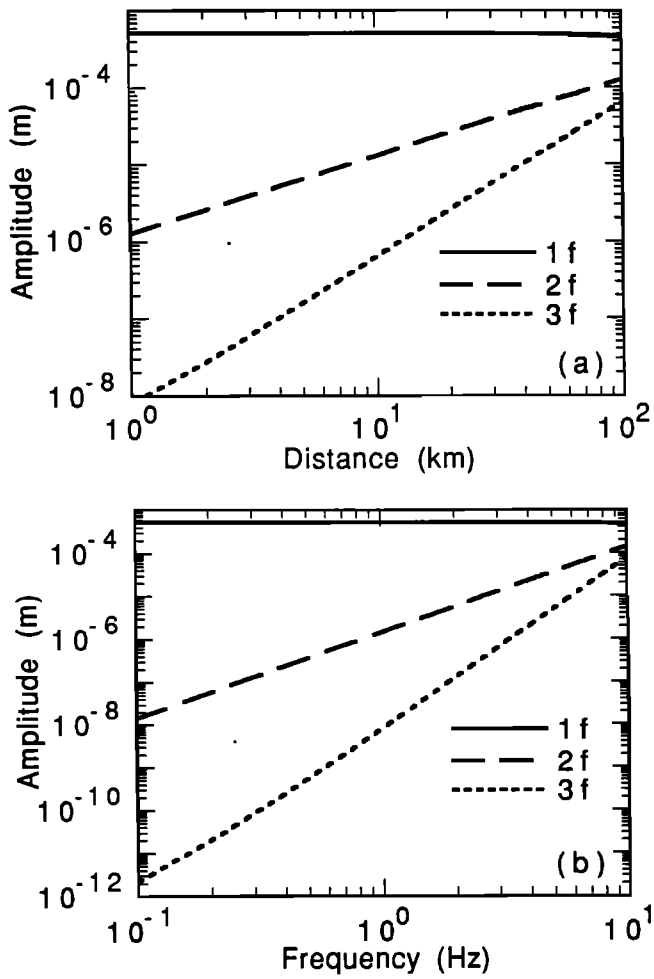

Figure 3. Displacement amplitudes for individual frequency components. Attenuation is not included. Solid curves are the amplitudes of the source frequency $1f$, long-dash curves are the amplitudes of the first harmonic $2f$, and short-dash curves are the amplitudes of the second harmonic $3f$. (a) Displacement amplitude as a function of propagation distance. The $1f$ amplitude decreases slightly, the $2f$ amplitude increases linearly with distance, and the $3f$ amplitude increases quadratically with distance. (b) Displacement amplitude as a function of source frequency at $x = 10$ km. The $1f$ amplitude decreases slightly, the $2f$ amplitude increases as the square of the frequency, and the $3f$ amplitude increases as the fourth power of the frequency.

as the external source [*Yu et al.*, 1992]. The transform of (38a) is

$$F(t) = \Omega t\, e^{-\Omega t}. \tag{38b}$$

As shown in Figure 4, this choice of external source is band limited in time and has a frequency spectrum that is flat for low frequencies and falls off as ω^{-2} for high frequencies.

In Figure 5 we show the displacement field as a function of frequency resulting from a source producing the frequency spectrum of (38a). We calculated the received frequency spectrum at four distances from the source ($x = 1$, 10, 20, and 40 km) with linear and first-order nonlinear terms taken into account, (25a) and (26a). Figure 5*a* shows the evolution of the frequency spectrum in the absence of attenuation. Figure 5*b* shows the evolution of the frequency spectrum where $Q \approx 100$. We chose τ, Δ, and ν such that the model Q is approximately equal to the measured Q in central California [*Mayeda et al.*, 1992]. The parameters used in the calculation are $\Omega = 40$ Hz, $U = 10^{-3}$ m (corresponding to strains of order 10^{-6}), $c_L = 6000$ m/s, $\beta = -10^3$ [*Meegan et al.*, 1993], $\Delta = 0.05$, $\nu = 1$, and $\tau = 0.3$ s. Clearly, higher frequencies are being created in the nonlinear interaction as a function of propagation distance. Note especially the decrease in the roll-off slope and corner frequency in Figure 5*b*. The amplitudes of sum and difference frequency components depend on the competition between growth with propagation distance due to nonlinearity and decay with distance due to attenuation. These results are in qualitative agreement with the numerical results of *Yu et al.* [1992] in a study of nonlinear soil response which concluded that nonlinearity enhances high frequencies at the expense of intermediate frequencies.

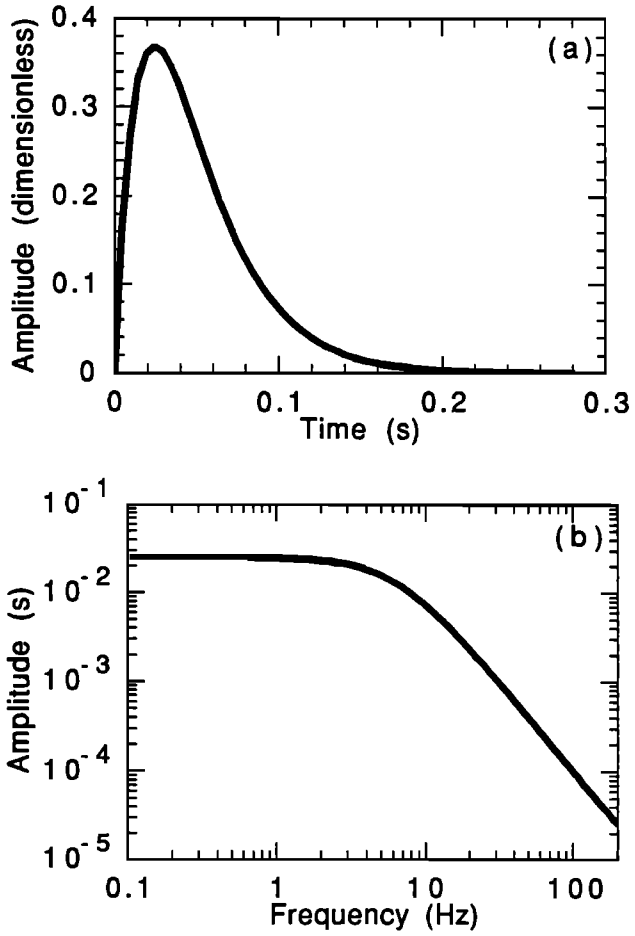

Figure 4. Broadband source function. (a) Time domain, (38b), $\Omega = 40$ rad. (b) Frequency domain, (38a). This source function is time limited and has a frequency spectrum that is flat at low frequencies and falls off as ω^{-2} at high frequencies, thereby providing a useful idealization of a seismic source.

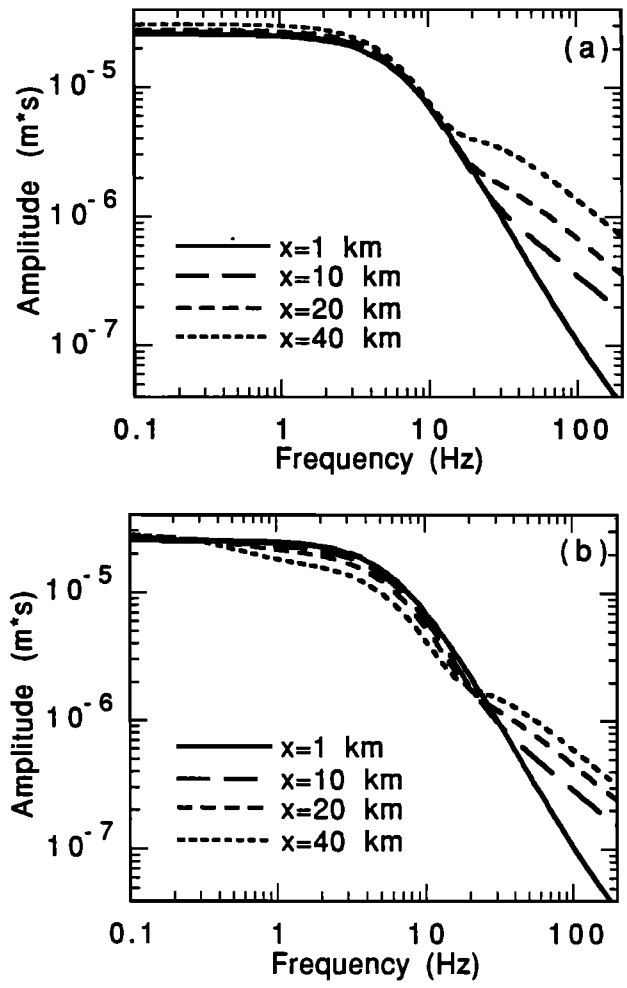

Figure 5. Displacement frequency spectrum of a broadband source, (38a). The pulse propagates to $x = 1$ km, 10 km, 20 km, and 40 km, progressively producing sum and difference frequencies through a first-order nonlinear interaction. (a) In the absence of attenuation; (b) including attenuation, $Q \approx 100$. The high-frequency contribution to the spectrum becomes more pronounced as the wave propagates.

Conclusions

In this paper we have developed and illustrated a theoretical framework for investigating the nonlinear interaction of frequency components in large-amplitude elas-

tic waves. We derived the equation of motion for the displacement field to third order in the strain, including attenuation by allowing the displacement derivative to have both instantaneous and retarded components. We solved the equation of motion by using the exact Green function solution to the linear problem and developing higher-order displacement components in terms of the exact solution. This method has conceptual clarity and a high degree of flexibility. It is a good approximation to an exact solution in cases where the energy shift due to nonlinear terms in the displacement is small (less than 10%), a limit that applies to many geophysical applications.

We have illustrated the use of the Green function technique in two examples.

(1) We solved analytically for the displacement field produced by a continuous single-frequency sine wave source to first order in the nonlinearity including attenuation and to second order in the nonlinearity in the absence of attenuation. We found that the first-order term, with components at twice the source frequency and at zero frequency, grows linearly with propagation distance and nonlinear coefficient and as the square of the initial displacement and source frequency. Asymptotically, the second-order term grows as the square of the propagation distance and the nonlinear coefficient and as the cube of the initial displacement and source frequency.

(2) We used a broadband frequency source to study the effect of first-order nonlinearity on seismic wave propagation. We found that frequencies above those in the original source are generated by the first-order nonlinear interaction in the rock. The high-frequency contribution to the total frequency spectrum becomes more pronounced as the wave propagates. After a few attenuation lengths, the frequency spectrum is dominated by attenuation. Thus the relative effects of attenuation and nonlinear interaction vary with distance from the source.

In the examples presented in this paper we used a single Green function, that of an infinite solid. Many other applications of the Green function technique are possible with other Green functions. For example, one could analytically solve for the Green function in a bounded medium, or one could use an empirical Green function derived from a suitable linear experiment. Given a Green function, solving for the displacement field to first order and higher in the nonlinearity is straightforward. In this manner, the important contributions to the nonlinearity may be studied independently of each other. The intent of this paper is to illustrate the breadth of the Green function technique. Careful application to physical situations is forthcoming.

Appendix: Attenuation

The driving force for the displacement field is the divergence of the stress field (1), and the stress field is a functional of the strain field (the spatial derivatives of the displacement). The intention of this appendix is to develop a model of the behavior of the system when the strain field (displacement derivative) is coupled to an internal degree of freedom of the system. Our interest is in materials like Berea sandstone that are known to have pervasive structural defects, such as microcracks and grain boundaries, which may be fully or partially saturated with fluid. Viewed on a length scale large compared to individual defects but small compared to a wavelength, we find that the system's displacement response to a force is delayed due to the coupling of the defects to the fluid. We model this delay in terms of a spatial derivative of the displacement that has instantaneous and retarded response. Thus, for example, we rewrite (6b) as

$$\rho\ddot{u}_y = \mu\frac{\partial}{\partial x}\left(\frac{\partial u_y}{\partial x} - \zeta_y\right) + S_y + (\lambda + 2\mu + m)\frac{\partial}{\partial x}\left[\left(\frac{\partial u_x}{\partial x} - \zeta_x\right)\left(\frac{\partial u_y}{\partial x} - \zeta_y\right)\right], \tag{A1}$$

where ζ is the dimensionless relaxation term governing the retarded response, satisfying

$$\tau\frac{\partial \zeta_i}{\partial t} + \zeta_i = \Delta\frac{\partial u_i}{\partial x}, \tag{A2}$$

and τ is the relaxation time [*Day and Minster*, 1984]. The coefficient Δ is in the range $0 \le \Delta \le 1$. It may be thought of as the fraction of the stress that is retarded and might be expected to scale with porosity or some measure of the defect density. For $\Delta = 0$, the system is not attenuative; for $\Delta = 1$, all of the stress field is retarded in time.

We solve for ζ in the frequency domain; therefore define $u_i(x,\omega)$ and $\zeta_i(x,\omega)$ such that

$$u_i(x,t) = \int \frac{d\omega}{2\pi} u_i(x,\omega)e^{-i\omega t}, \tag{A3}$$

$$\zeta_i(x,t) = \int \frac{d\omega}{2\pi} \zeta_i(x,\omega)e^{-i\omega t}. \tag{A4}$$

Then from (A2)

$$\zeta_i(x,\omega) = \frac{\Delta}{1 - i\omega\tau}\frac{\partial u_i(x,\omega)}{\partial x}, \tag{A5}$$

$$\frac{\partial u_i(x,\omega)}{\partial x} - \zeta_i(x,\omega) = \left(1 - \frac{\Delta}{1 - i\omega\tau}\right)\frac{\partial u_i(x,\omega)}{\partial x}. \tag{A6}$$

With the addition of an arbitrary power of $\omega\tau$, the coefficient of the displacement derivative on the right-hand side of (A6) is the χ defined in (9).

We do not believe that this model has a deep connection to what is actually taking place in the system. Rather, we wish to model the essential elements of the behavior of the system in a way that is qualitatively correct. Further, we do not expect that a single relaxation time τ or a single retarded fraction Δ will suffice for careful modeling of real systems [*Day and Minster*, 1984]. One may develop an effective medium theory of the linear behavior of the system yielding suitable $\tau(\omega)$ and $\Delta(\omega)$ for such purposes.

Acknowledgments. The author thanks R. A. Guyer, P. A. Johnson, G. D. Meegan, Jr., S. Kostek, R. J. O'Connell, and I. A. Beresnev for helpful discussions. T. J. Shankland, R. P. Swift, and J. R. Kamm made valuable comments on the manuscript. This research is supported by the Office of Basic Energy Science, Engineering and Geoscience under contract W7405-ENG-36 and the U.S. Department of Energy, Office of Arms Control and Nonproliferation, under contract ST604.

References

Day, S. M., and J. B. Minster, Numerical simulation of attenuated wavefields using a Padé approximant method, *Geophys. J. R. Astron. Soc., 78,* 105-118, 1984.

Gol'dberg, Z. A., Interaction of plane longitudinal and transverse elastic waves, *Sov. Phys. Acoust., 6,* 306-310, 1960.

Green, R. E., Jr., *Treatise on Materials Science and Technology,* vol. 3, *Ultrasonic Investigation of Mechanical Properties,* pp. 73-83, Academic, San Diego, Calif., 1973.

Landau, L. D., and E. M. Lifshitz, *Theory of Elasticity,* 3rd ed., pp. 104-107, Pergamon, New York, 1959.

Mayeda, K., S. Koyanagi, M. Hoshiba, K. Aki, and Y. Zeng, A comparative study of scattering, intrinsic, and coda Q^{-1} for Hawaii, Long Valley, and central California between 1.5 and 15.0 Hz, *J. Geophys. Res., 97,* 6643–6659, 1992. (Correction, *J. Geophys. Res., 97,* 12,425, 1992.)

Meegan, G. D., Jr., P. A. Johnson, R. A. Guyer, and K. R. McCall, Observations of nonlinear elastic wave behavior in sandstone, *J. Acoust. Soc. Am.,* in press, 1993.

Murnaghan, F. D., *Finite Deformation of an Elastic Solid,* pp. 60-66, John Wiley, New York, 1951.

Nazarov, V. E., L. A. Ostrovsky, I. A. Soustova, and A. M. Sutin, Nonlinear acoustics of micro-inhomogeneous media, *Phys. Earth Planet. Inter., 50,* 65-73, 1988.

Nowick, A. S., and B. S. Berry, *Anelastic Relaxation in Crystalline Solids,* pp. 46-57, Academic, San Diego, Calif., 1972.

O'Connell, R. J., and B. Budiansky, Measures of dissipation in viscoelastic media, *Geophys. Res. Lett., 5,* 5-8, 1978.

Polyakova, A. L., Nonlinear effects in a solid, *Sov. Phys. Solid State, 6,* 50-54, 1964.

Yu, G., H. G. Anderson, and R. Siddharthan, On the characteristics of nonlinear soil response, *Bull. Seismol. Soc. Am., 83,* 218-244, 1992.

K. R. McCall, Earth and Environmental Sciences Division, Mail Stop D443, Los Alamos National Laboratory, Los Alamos, NM 87545.

(Received April 30, 1993; revised October 8, 1993; accepted October 20, 1993.)